Mapping the holes: 3D ISM maps and diffuse X-ray background

R. Lallement[1], J.-L. Vergely[2], L. Puspitarini[3], S. Snowden[4],

M. Galeazzi[5], and D. Koutroumpa[6]

[1] GEPI Observatoire de Paris, PSL Research University, CNRS, Univ Paris Diderot, Sorbonne Paris Cité, Place Jules Janssen 92190 Meudon, France, e-mail: `rosine.lallement@obspm.fr`
[2] ACRI-ST, 260 route du Pin Montard, Sophia Antipolis, France
[3] Bosscha Observatory and Department of Astronomy, FMIPA, Institut Teknologi Bandung, Jl. Ganesha 10, Bandung 40132, Indonesia
[4] NASA/Goddard Space Flight Center, Greenbelt, MD 20771, USA
[5] Department of Physics, University of Miami, Coral Gables, Florida 33124, USA
[6] LATMOS, Université de Versailles Saint Quentin, INSU/CNRS, 78200 Guyancourt

Abstract. 3D maps of Galactic interstellar dust and gas reveal empty regions, including cavities carved by stellar winds and supernovae. Such cavities are often filled with hot gas and are sources of soft X-ray background emission. We discuss the combined analysis of the diffuse soft (0.25 keV) X-ray background and the 3D distribution of nearby ($\leq$1 kpc) dust, including studies of shadows cast by nearby clouds in the background. This analysis benefits from recent progress in the estimate of the foreground X-ray emission from the heliosphere. New and past X-ray data are found to be consistent with the maps if the $\simeq$ 100-150 pc wide Local Bubble surrounding the Sun is filled with 10^6K gas with a pressure 2nT $\simeq$ 10,000 K cm^{-3}. On the other hand, the giant cavity found in the 3rd Galactic quadrant has a weaker volume emission than the LB and is very likely filled to a large extent with warm ionized gas. Its geometry suggests a link with the tilted Gould belt, and a potential mechanism for the formation of the whole structure has been recently proposed. According to it, the local inclination of gas and stars, the velocity pattern and enhanced star formation could have been initiated 60-70 Myr ago when a massive globular cluster crossed the Galactic Plane in the vicinity of the Sun. The destabilization of stellar orbits around the Sun may have generated enhanced asteroid falls of the Cretaceous-Tertiary (KT) extinction events. Additionally, a short gamma ray burst may have occurred in the cluster during the crossing, producing intense ionization and subsequent shock waves leading to the star formations seen today in the form of the giant ionized region and OB associations at its periphery. Gaia measurements of nearby stars and clusters should help shedding light on the local history.

Key words. Galaxy:Interstellar medium - Galaxy:Globular clusters

1. Introduction

3D maps of the nearby and distant ISM have been produced based on various stellar data, mainly photometric extinction but also diffuse interstellar bands (DIBs) and gaseous species lines (Marshall et al., 2006; Vergely et al., 2010; van Loon et al., 2013; Welsh et al., 2010; Lallement et al., 2014b; Schlafly et al., 2014; Sale et al., 2014; Kos et al., 2014; Schultheis et al., 2014; Zasowski et al., 2015; Green et al., 2015, and references from this volume). Various methods have been used to synthesize the distance-limited data, including full 3D tomographic inversion (Tarantola & Valette, 1982; Vergely et al., 2001; Sale & Magorrian, 2014). During the next years maps of increasing quality should be produced, thanks to continuing or new stellar surveys on one hand, and precise Gaia parallaxes on the other hand.

3D maps reveal clouds and cavities. Because cavities are often hot gas bubbles blown by stellar winds and supernovae their distance assignments are helpful for a better understanding of the star formation cycles. Moreover, because hot gas bubbles emit in the soft X-ray band, inter-comparing X-ray diffuse emission and 3D cavities becomes a tool to assign distance to the hot gas and to constrain its physical properties. Here we focus on the local, low resolution 3D dust maps of of the solar neighborhood ISM of Lallement et al. (2014b) (hereafter LVVPEC) that were obtained through inversion of color excess measurements of only 23,000 target stars, a brightness-limited photometric dataset. As a consequence of this limitation these maps are strongly influenced by biases towards low-extinction lines-of-sight, disfavoring a good representation of regions beyond opaque clouds. On the contrary, cavities are well revealed, simply through their enhanced volume density of observed targets. We illustrate how the inter-comparison between the 3D maps and the soft X-ray surface brightness sky maps allow the determination of some physical properties of the hot gas in the cavities, and how the knowledge of locations and properties of the cavities may shed light on the local interstellar and stellar history.

2. The nearest HOLE: the Local Bubble

The Local Cavity or Local Bubble (LB) is a void within the H I gas of the Galactic disk surrounding the Sun. It extends from a few tens of parsecs in the Galactic plane to 200 pc or more at high Galactic latitudes. For a long time the soft-X-ray background (SXRB) emission observed at 1/4 keV with the ROSAT satellite has been attributed entirely to hot gas filling the LB (see, e.g., Snowden et al. (1997) for more details). As a matter of fact one optical depth at this wavelength is about 10^{20} H atoms cm^{-2}, i.e. most of the observed emission has to be local. The more recent discovery of the solar wind charge-exchange X-ray emission (Cravens, 2000) has been challenging this unique origin, and in particular the fraction of the background originating within the LB hot gas for directions close to the Plane has been considered as small and even potentially null (Koutroumpa et al , 2009). The charge-exchange emission is produced in the Earth's magnetosphere and in the heliosphere and it varies with time in response to solar wind variations, on hourly scales for the magnetosphere and daily to yearly scales for the heliosphere. Making use of this variability a fraction of the solar wind contamination was already removed from ROSAT count rates during the *cleaning* process. However due to the different time scales and the many parameters governing the charge-exchange such as the relative ionic abundances and latitudinal anisotropies it has been particularly difficult to assess the remaining contribution. The situation remained unclear until recently, due to all of the uncertainties, and also the weakness of the signal.

In the last two years new measurements of the solar wind charge-exchange diffuse X-ray background and also improved models of this signal have provided better constraints and strong support for the existence of hot gas emission from all directions, including the Plane. First, dedicated rocket data have been obtained by Galeazzi et al. (2014), showing in a very convincing way that the total residual solar wind charge-exchange contribution in the ROSAT survey was approximately 40 per
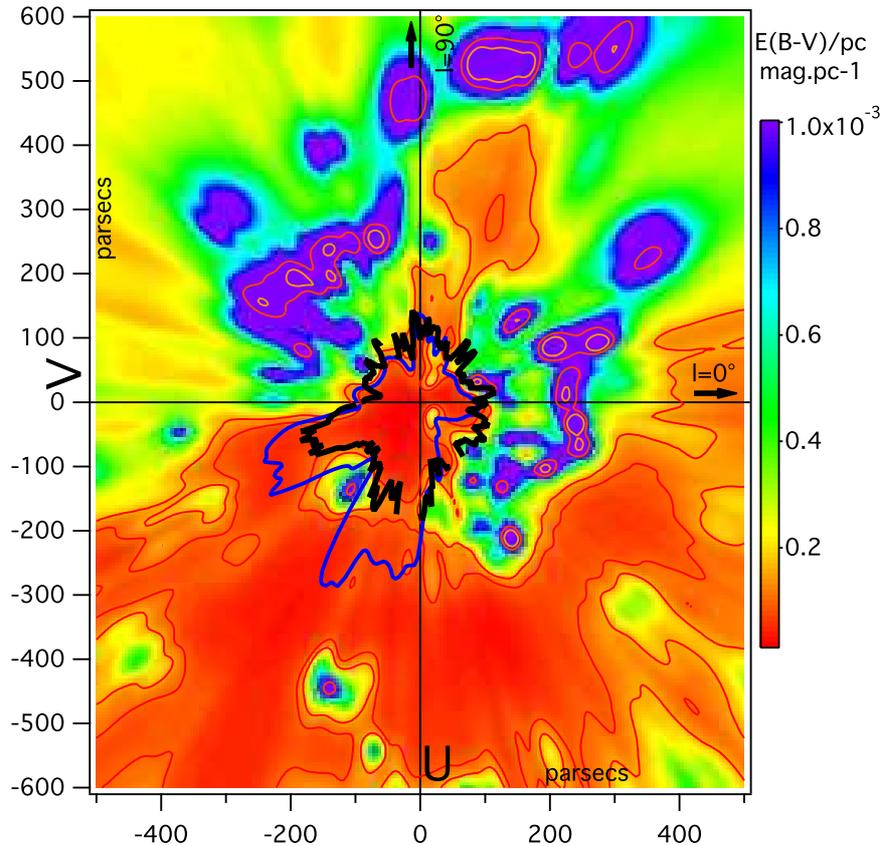
Fig. 1. Differential color excess in the Galactic plane in the vicinity of the Sun, derived by inversion of line-of-sight data. The Sun is at (0,0) and the Galactic center direction is to the right. The main dense cloud complexes (blue-violet areas) belong to the Gould belt. Cavities (in red) include the Local Bubble around the Sun. The black thick line is a Sun-centered polar plot of the 1/4 keV X-ray surface brightness measured by ROSAT, after subtraction of a modeled charge-exchange contribution. The scaling is chosen in such a way that the curve coincides with the LB contour in the second and fourth quadrants. The violet curve is a similar polar representation of the surface brightness computed by means of a simplified radiative transfer model, assuming cavities are all homogeneously filled by emitting 1MK hot gas and all dense clouds are absorbing the radiation. Optical thicknesses are assumed proportional to the dust columns. Figure from (Puspitarini et al., 2014)

cent of the 1/4-keV flux in the Galactic plane. A very good agreement was found with previous data, when taking into account the respective geometries and solar wind properties, and using the same improved model of the solar wind charge-exchange emission. A second line of evidence came from the comparison between the ROSAT background data and the interstellar dust distribution in the Sun vicinity. Based on the LVVPEC 3D low resolution map, Puspitarini et al. (2014) computed a simplified radiative transfer model of the 1/4 keV radiation. They assumed that all regions devoid of dust (the cavities) are filled with homogeneous hot gas at 1 million K and are the source of X-ray emission. All regions found

to be filled with dense IS dust were assumed to be absorbing clouds with hydrogen columns proportional to the dust columns. The resulting pattern of the emission from the Plane detected at the Sun is shown in polar coordinates in Fig 1, superimposed on a planar cut within the 3D distribution. The scaling for the X-ray surface brightness is chosen in such a way that the polar curve coincides with the LB contour in the second and fourth quadrants. In parallel, ROSAT data recorded within the Plane were retrieved and for each direction a foreground solar wind charge-exchange emission was subtracted, based on the model presented in Lallement (2004) and scaled to match the recent determination from Galeazzi et al. (2014) and Snowden et al. (2014). The comparison between the observed emission attributable to the hot gas and the modeled emission from the simplified radiative transfer code reveals interesting similarities, with coinciding enhancements from several regions (longitude intervals ≃ 0-10, 75-90, 190-210 and 230-270 degrees). On the other hand the comparison between the data and the LB geometrical contours also reveals similarities that strongly suggest a volume-distributed source, the LB. In the third quadrant it appears clearly that the two *lobes* at 190-210 and 230-270 degrees longitude are X-ray enhancements generated within the giant cavity, and that the weaker emission region (depression region) around ≃ 225 degrees longitude corresponds to the shadow cast by the cloud complex located at 200 pc distance in this direction. This again favors emission from within the Plane, both from the LB and from neighboring cavities. Equating the data and the model and assuming homogenous hot gas at 1 MK and solar metallicity implies a hot gas pressure nT of ≃ 10,000 cm^{-3}K.

Additional strong evidence came from the use of shadowing by distinct clouds in the interstellar medium to separate the observed intensity into foreground and background components, relative to the cloud. Snowden et al. (2015) used the cold and close Leo cloud, and Snowden et al. (2015) used a high latitude filamentary cloud possessing a well bracketed distance of 98 ± 6 pc (Puspitarini & Lallement, 2012). Assuming homogenous hot gas, they derived the same average hot plasma pressure in front of the clouds. Moreover, they used ROSAT measurements towards 14 additional directions at low and intermediate latitudes where the local 3D maps show that opaque clouds block any background radiation (100% shadowing) at the LB boundary. All measurements were consistent with the same average pressure and X-ray emissivity determined in Puspitarini et al. (2014) and Snowden et al. (2014) (see Snowden et al. (2015) for more details).

In summary, all these recent advances self-consistently point to the existence of hot gas in the LB and beyond, including within the Plane, with an inferred pressure of the LB hot gas significantly smaller than derived before the discovery of the foreground solar wind charge exchange contamination. Apart from the rocket data analysis, the new analyses have required the use of the 3D maps of the local ISM, which demonstrates their usefulness with respect to the physical state of the ISM.

3. The nearest SUPERHOLE: GSH238+00+09

The map shown in Fig 1 reveals the series of dense structures that bound the Local Cavity, namely the Aquila, Ophiuchus, Scorpius, Lupus, Crux and Centurus dense clouds in the first and fourth quadrant, and the Cassiopeia, Lacerta, Perseus, Taurus, and the closest Orion clouds in the anti-center area. Since most of these structures are not centered exactly on the Plane, what appears in the horizontal cut in the distribution are their top or bottom parts. These well known structures are part of the Gould belt (GB), a ≃ 20° inclined, roughly ellipsoidal chain of dense clouds and young (≤10 Myr old) O-B associations. Two types of scenarios have been developed to explain the expanding and rotating Gould belt, the oblique impact of a massive external cloud or a series of explosive events, potentially initiated by a major one, such as a gamma-ray burst (Olano, 2001; Perrot & Grenier, 2003; Pöppel et al., 2010).

In addition to the Gould belt clouds Fig 1 also shows in the third quadrant a conspicuous, 500 to 1,000 pc wide cavity. This cavity can
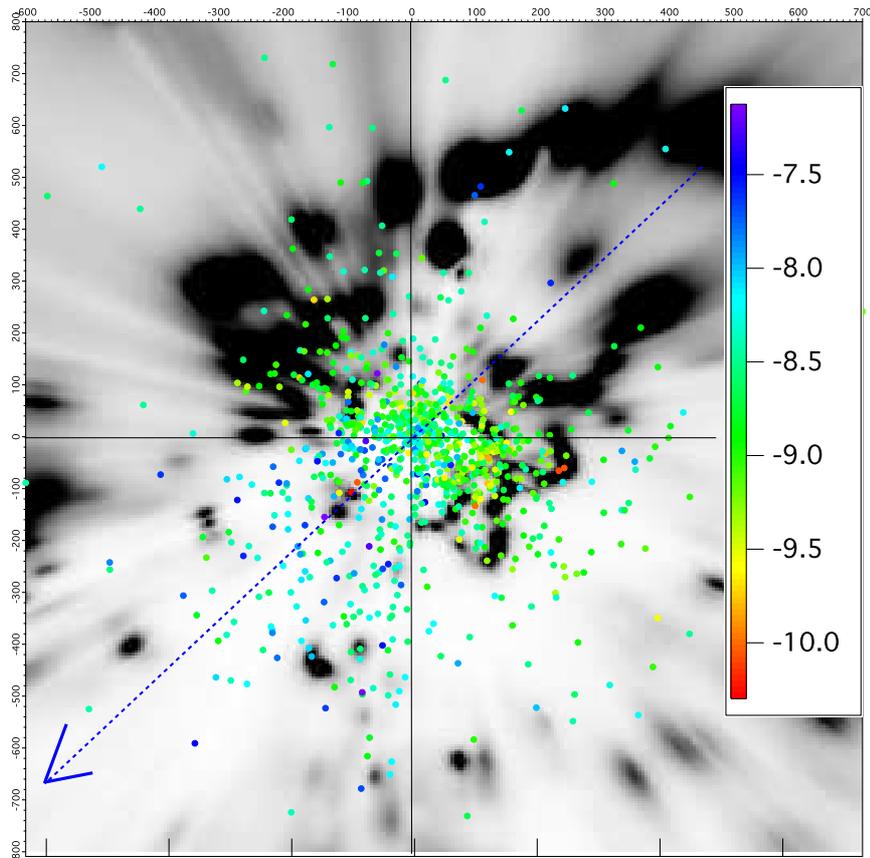
Fig. 2. CaII target stars close to the GP, superimposed on the opacity map of Fig 1 (from Puspitarini et al. 2014). The color refers to the ratio between the CaII column-density measured by absorption and the color excess along the same line-of-sight, derived by line-of-sight integration through the inverted 3D distribution of differential opacity. Stars located in the third quadrant are characterized by a particularly high CaII/E(B-V) ratio.

be seen as an extension to large distances of the so-called Canis Major *tunnel*, a region of rarefied gas that extends up to 130-150 pc in the direction of Canis Major (Gry et al., 1985). The new, huge cavity is centered below the Plane (see the various planar cuts in LVVPEC), and its location and extent correspond remarkably well to the super-shell GSH238+00+09 (HI 21cm observations) discovered by Heiles (1998). This peculiar super-bubble is bounded on one side by a chain of clouds in the direction of Orion, and by the Vela clouds at $\simeq$ 260-270 °. When looking at the whole struc-

ture of the Gould belt clouds and the giant cavity, it is striking that they seem to share the same long axis, as if they were resulting from a common event operating at a very large-scale and characterized by a specific orientation (Lallement et al., 2014a). Interestingly, the model devised by Olano (2001) to reproduce the Gould belt predicts such a cavity lagging beyond the belt, which reinforces strongly such a model. However, as noted by Lallement (2015), despite its many advantages the supercloud model implies a puzzling coincidence, namely that elemental abundances in

the super-cloud gas and stars prior to the encounter with the disk were identical to abundances in the disk. As a matter of fact, there is a clear absence of inhomogeneities in the chemical abundances in the local gaseous ISM (e.g., O/H is about constant, see André et al. 2003, and carbon shows little variability, see Sofia et al. 2004), and there are no abundance differences among the nearby stars in relation with their kinematics (Nieva & Przybilla, 2012). A second observation disfavors the super cloud model. It predicts a large cavity devoid of any interstellar matter. But in what follows we argue that the third quadrant cavity is very largely filled with ionized gas. There are several arguments for that.

First, it has been known for a long time that there is significant interstellar HII gas in this direction, as demonstrated by Gry et al. (1985) based on UV spectra of the star β CMa at $\simeq$ 150 pc, a star located between the LB and the 3rd quadrant cavity. This was also noted by Snowden (1998) who also used available absorption data and suggested that the cavity has large amounts of ionized gas. Second, a general ionization gradient of the IS matter along an axis pointing from this region has been derived by Wolff et al. (1999) based on EUVE spectra of white dwarfs. Extrapolating from this gradient into the large cavity implies fully ionized gas beyond 200 pc. Third, Fig 1 shows that if the giant cavity was filled with hot gas similar to the one in the LB the 1/4 keV brightness should be much more intense than from other directions and the polar curve should extend much farther than what is seen. Instead the two *lobes* mentioned above are less than twice as long than the average distance in other quadrants. This implies that either the hot gas pressure is smaller or another type of gas is present, dust-poor warm ionized gas being a likely possibility. A fourth, more quantitative diagnostic is shown in Fig 2 (from Puspitarini et al., 2014). These authors used all target stars with available ionized calcium column and Hipparcos distances. They estimated the reddening to each star by integrating along the path to the target though the LVVPEC differential color excess distribution and computed the ratio between the CaII column and the in-

tegrated color excess. Fig 2 shows this ratio for all stars that are closer to the Plane than 100 pc. Obviously the CaII to dust ratio is much higher in the cavity, with an average ratio at least one order of magnitude above the mean in the three other quadrants. It is well known that in shocked and heated gas dust grains are evaporated and calcium is released in the gas phase, two effects that both contribute to increase the CaII to dust ratio. Very likely the two effects are at play here and since the measured ratio is typical of warm HII gas it is very likely that all the CaII is tracing such gas. For stars located in the third quadrant at $\simeq$ 300 pc or more, CaII columns reach 10^{12} to 10^{13} cm^2. Approximate conversions to cloud sizes can be done using average CaII to H values found for the local clouds (see e.g., Redfield & Linsky, 2000). Conversion distances are between 100 and 1000 parsecs, confirming that a large fraction of the sightline towards the stars is probably filled by warm ionized gas and not hot X-ray emitting gas.

4. A potential scenario for the formation of the Gould belt and the GSH238+00+09 superbubble

Massive compact globular clusters (GCs) orbiting the Milky Way (MW) are regularly crossing the Plane, and the effect of those crossings has been mainly studied from the point of view of the evolution of the cluster itself. Very little has been done on the impact the crossings may have on the MW gas and stars, as the impacts of the clusters are unimportant in comparison with dwarfs galaxies or dark matter subhalos. However the most massive ones must have a non-negligible impact, especially at spatial scales on the order of 500pc-1 kpc and it has been suggested that the Gould belt and potentially the 3rd quadrant cavity may result from such a crossing (Lallement, 2015). A prototype of massive and compact GCs is 47 Tucanae (47 Tuc). Presently located at 4.5 kpc from the Sun and far below the Galactic plane (galactic coordinates (l,b) = (306, -45)), its estimated mass is 1-2 million solar masses, for a diameter of 40 pc. The MW stellar surface density being on the order of 50

solar masses pc^2 in the Sun vicinity (Holmberg & Flynn , 2004), the mass of 47 Tuc is equivalent to the mass of a MW cylinder with a 200 pc diameter. On the other hand, the relative velocity between the GC and the Sun for the orbits of close approach is on the order of 100 km s^{-1} (Dinescu et al., 1999), with a vertical component on the order of 50 km s^{-1}, while the average vertical velocity of the MW stars is on the order of 15-20 km s^{-1}. The simple comparison of momenta shows that a crossing will locally generate fairly significant perturbations. The size of the impacted area can be estimated based on the free particle approximation formula (2) of Widrow et al. (2014). According to this formula and for the above parameters, a mid-plane star is affected by a strong scattering (90 degrees) for an impact parameter of the cluster on the order of 600 pc, meaning that the size of the impacted area is on the order of about this distance, i.e. on the same order as the size of the Gould belt or the whole structure seen in Fig 1. Widrow et al. (2014) computed the influence of the vertical velocity of the crossing object on subsequent oscillations. For the solar neighborhood and 50 km.s^{-1} vertical velocity their models show that the impacted area could be in a intermediate state between a simple bending-mode and higher-order modes, suggesting that a pronounced warp similar to the Gould plane structure is potentially formed after the crossing of a GC of the type of 47 Tuc.

Perrot & Grenier (2003) have calculated that the Gould belt gas oscillation time is on the order of 50 Myr. This implies that the time elapsed since the crossing must be on this order, since no strong dissipation has occurred yet. This is also in agreement with the ages of the Gould belt stars that range from 20 Myr for the brightest massive objects of the main associations to up to 60-80 Myr, as shown by Torra et al. (2000); Guillout et al. (1998) and open cluster analyses (Bobylev, 2006). If young associations have been formed as a result of dynamical perturbations after the crossing, those age are in agreement with a triggering event $\simeq$ 70 Myr ago. Domainko et al. (2013) have extrapolated back the orbits of the most massive GCs based on their currently observed 3D-space velocities (Dinescu et al., 1999) and the solar orbital parameters (Dehnen & Binney , 1998). Their study was motivated by the recent suggestion that massive ultra-dense GCs are the main sources of short and hard gamma ray bursts (SGRBs), the bursts being associated with merging neutron star binaries (see, e.g., Gehrels et al., 2009), and that following this idea GC crossings with the Plane close to the Sun could have been the triggering events for mass extinctions on Earth (e.g., Melott & Thomas (2011)). Domainko et al. (2013) found that 47 Tuc may have crossed the MW plane close to the Sun at 70, 180 and 340 Myr, the first date evidently corresponding to the famous KT extinction. If this crossing occurred 70 Myr in the past, it must have produced significant perturbations in the local stars and ISM, independently of the occurrence of a SGRB. Indeed, it could have destabilized Oort cloud objects and triggered the infall of comets and meteorites (Montmerle, 2014), subsequently producing the KT extinction without the need for any SGRB.

There are however several arguments in favor of a SGRB. One is the existence of the large amount of ionized gas within the giant cavity, a second is its distribution over large distances, a third is the associated strong dust depletion, and a fourth is the ionization gradient and the significant helium ionization state (Wolff et al., 1999). At variance with long GRBs that occur in molecular clouds and strongly ionize their surrounding dense gas (see, e.g. Krongold & Prochaska, 2013), the radiation from the short GRBs is entirely available for ionization of gas distributed much farther away. With a number of ionizing photons on the order of up to 10^{58} (assuming that the total radiation output of a short GRB is 1000 times less intense than the one of a long GRB and for long GRB numbers taken from Krongold & Prochaska 2013), the burst is able to quasi-instantaneously ionize H column-densities on the order of 5 10^{20} cm^2 in two cones of less than 50 deg opening angle each, i.e. columns similar to those of the ionized gas within the 3rd quadrant cavity as discussed above. The effect on the dust must be quite strong too. Such a GRB must be very effective

in destroying the dust, especially in low- density environments and for the smaller grains. Crude estimates show that 0.1 micron grains will be evaporated over hundreds of pc in locations where the radiation is not fully attenuated by the interaction with the gas. Note that if grains are enriched in deuterium, such processes may affect the D/H ratio in the gaseous phase through inhomogeneous release of D during the destruction, following the mechanism suggested by Linsky et al. (2006). For all these reasons it is tempting to associate the GSH238+00+09 ionized and dust-poor cavity with a radiation burst. In this case, the ionization gradient (arrow in Fig 2) points to an ionizing source that is today within the 3rd quadrant cavity. Since the Sun and the ISM have moved independently, extrapolating back their motions would require specific models. A crude approximation consists in assuming that both the Sun and the bulk of the ISM have been moving in the same way within the Local Standard of Rest (LSR). Indeed, interstellar absorption line Doppler shifts in the spectra of stars within 500 pc allow to determine the motion of the Sun with respect to the bulk of the IS gas, and this motion today is found to be very similar in direction and modulus to the motion of the Sun in the LSR. Assuming those motions w.r.t. the LSR have been about constant over the last 65 Myr and extrapolating back the Sun's location using the most recent value of the Solar motion of Schönrich et al. (2010), this places the Sun 60 Myr ago at a distance of 1200 pc and coordinates (l, b)= (228, -23) w.r.t. the present coordinate system. This location corresponds to the extremity of the third quadrant cavity. Again specific dynamical models of stars and clouds are needed to go further. Improved 3D maps are also strongly needed to build a convincing scenario in a more qualitative way.

the soft X-ray background has recently produced significant results and especially has helped to solve a long-standing debate about the existence and the pressure of hot interstellar gas within the cavity close to the Plane. The main conclusion is that, in spite of the large contamination of the cosmic X-ray background at low latitudes by foreground solar wind charge-exchange diffuse X-ray emission, a large fraction of the emission is due to surrounding hot gas and all results converge to a LB hot gas pressure on the order of 10,000 K cm^{-3} (for more details see the various results of Galeazzi et al. (2014); Puspitarini et al. (2014); Snowden et al. (2014), Snowden et al.(2015a,b).

Maps reveal a giant cavity in the 3rd quadrant that has been identified with the volume bounded by the supershell GSH 238+00+09 detected by Heiles (1998). Combining with the soft X-ray background and various absorption data, we argue that this cavity is largely filled with warm ionized gas where dust has been evaporated. This cavity seems to be geometrically related to the Gould belt of stars and clouds, and this apparent link has motivated a new scenario for the history of the local ISM. A mechanism recently suggested by Lallement (2015) attributes the formation of the Gould belt and potentially the large cavity to the impact of the MW crossing by a massive globular cluster about 60-70 Myr ago, and possibly to a short gamma ray burst within the cluster at about the time of crossing. The compact and massive cluster 47 Tuc, whose orbital parameters have been shown by Domainko et al. (2013) to be compatible with a crossing at this date at limited distance from the Sun, is one of the most serious candidates. Gaia astrometric and chemo-dynamical results for MW stars are needed to reinforce or dismiss this hypothesis.

5. Conclusion

3D maps of the ISM are important tools in various respects. Here we have focused on one of those aspects, the detection of cavities.

In the case of the local cavity, the Local Bubble, the comparison between 3D maps and

References

André, M. K., Oliveira, C. M., Howk, J. C., et al. 2003, ApJ, 591, 1000

Bobylev, V. V. 2006, Astrophys. Lett., 32, 816

Cravens, T.E., ApJ, 532, L153

Dehnen, W., & Binney, J. J. 1998, MNRAS, 298, 387

Dinescu, D. I., Girard, T. M., & van Altena, W. F. 1999, AJ, 117, 1792

Domainko W., Bailer-Jones, C.A.L., Feng F. 2013, MNRAS, 432, 258

Galeazzi, M., Chiao, M., Collier, M. R., et al. 2014, Nature, 512, 171

Gehrels, N., Ramirez-Ruiz, E., & Fox, D. B. 2009, ARA&A, 47, 567

Green, G. M., Schlafly, E. F., Finkbeiner, D. P., et al. 2015, ApJ, 810, 25

Gry, C., York, D. G., & Vidal-Madjar, A. 1985, ApJ, 296, 593

Guillout, P., et al. 1998, A&A, 337, 113

Heiles, C. 1998, ApJ, 498, 689

Holmberg, J., & Flynn, C. 2004, MNRAS, 352, 440

Kos, J., Zwitter, T., Wyse, R., et al. 2014, Science, 345, 791

Koutroumpa, D., et al. 2009a, ApJ, 696, 1517

Krongold, Y., & Prochaska, J. X. 2013, ApJ, 774, 115

Lagarde, N., Romano, D., Charbonnel, C., et al 2012, A&A, 542, A62

Lallement, R., et al. 2003, A&A, 411, 447

Lallement, R. 2004, A&A, 418, 143

Lallement, R., Hébrard, G., & Welsh, B. Y. 2008, A&A, 481, 381

Lallement, R., et al. 2014, A&A, 561, A91 (LVVPEC)

Lallement, R., Vergely, J.-L., & Puspitarini, L. 2014, MmSAI, 85, 339

Lallement, R. 2015, Journal of Physics Conference Series, 577, 012016

Linsky, J. L., Draine, B. T., Moos, H. W., et al. 2006, ApJ, 647, 1106

Marshall, D. J., et al. 2006, A&A, 453, 635

Melott, A. L., & Thomas, B. C. 2011, Astrobiology, 11, 343

, Montmerle T., private comm.

Nieva, M.-F., & Przybilla, N. 2012, A&A, 539, A143

Olano, C. A. 2001, AJ, 121, 295

Perrot, C. A., & Grenier, I. A. 2003, A&A, 404, 519

Pöppel, W. G. L., et al. 2010, A&A, 512, A83

Puspitarini, L., & Lallement, R. 2012, A&A, 545, A21

Puspitarini, L., Lallement, R., Vergely, J.-L., & Snowden, S. L. 2014, A&A, 566, A13

Redfield, S., & Linsky, J. L. 2000, ApJ, 534, 825

Sale, S. E., Drew, J. E., Barentsen, G., et al. 2014, MNRAS, 443, 2907

Sale, S. E., & Magorrian, J. 2014, MNRAS, 445, 256

Schlafly, E. F., Green, G., Finkbeiner, D. P., et al. 2014, ApJ, 789, 15

Schönrich, R., Binney, J., & Dehnen, W. 2010, MNRAS, 403, 1829

Schultheis, M., Chen, B. Q., Jiang, B. W., et al. 2014, A&A, 566, A120

Snowden, S. L., Egger, R., Freyberg, M. J., et al. 1997, ApJ, 485, 125

Snowden, S. L. 1998, in The Local Bubble and Beyond, IAU Colloq. 166, eds. Breitschwerdt, Dieter et al. (Springer, Berlin), Lecture Notes in Physics, 506, 103

Snowden, S. L., Chiao, M.,Collier, M.R., et al. ApJ, 791, L14

Snowden, S. L., Heiles, C., Koutroumpa, D., et al. 2015, ApJ, 806, 119

Snowden, S. L., Koutroumpa, D., Kuntz, K. D., Lallement, R., & Puspitarini, L. 2015, ApJ, 806, 120

Sofia, U. J., et al. 2004, ApJ, 605, 272

Tarantola, A., & Valette, B. 1982, Reviews of Geophysics and Space Physics, 20, 219

Torra, J., Fernández, D., & Figueras, F. 2000, Astron. & Astrophys., 359, 82

van Loon, J. T., Bailey, M., Tatton, B. L., et al. 2013, A&A, 550, A108

Vergely, J.-L., et al. 2001, A&A, 366, 1016

Vergely, J.-L., et al. 2010, A&A, 518, A31

Welsh, B. Y., et al. 2010, A&A, 510, A54

Widrow, L. M., et al. 2014, MNRAS, 440, 1971

Wolff, B., Koester, D., & Lallement, R. 1999, A&A, 346, 969

Zasowski, G., Ménard, B., Bizyaev, D., et al. 2015, ApJ, 798, 35